Engineering xxx (xxxx) xxx

Contents lists available at ScienceDirect

Engineering

journal homepage: www.elsevier.com/locate/eng

Research
Intelligent Manufacturing—Article

Quasi-Static Hypergraph Neural Networks: A High-Performance Approach for Digital Twin Modeling of Manufacturing Process Systems with Dynamic Performance Evolution

Yiru Chen [#], Peiyuan Ding [#], Jianfu Zhang, Pingfa Feng, Xiangyu Zhang, Jianjian Wang [*]

State Key Laboratory of Tribology in Advanced Equipment, Department of Mechanical Engineering, Tsinghua University, Beijing 100084, China

ARTICLE INFO

Article history:
Received 12 July 2025
Revised 27 February 2026
Accepted 6 March 2026
Available online xxxx

Keywords:
Hypergraph neural networks
Digital twin
Manufacturing process systems
Dynamic performance evolution

ABSTRACT

Variations in product quality often originate from dynamic changes in the performance of manufacturing process systems. Developing digital twin models for model-based process control and optimization is a key strategy for improving quality; however, this approach is often constrained by the high cost of data acquisition in industrial environments. To address this challenge, this study proposes a quasi-static hypergraph neural network (QS-HGNN) model framework. Grounded in the assumption of microscopic quasi-static behavior and macroscopic evolution in process system performance, the proposed method abstracts process elements as nodes and uses hypergraph topology to represent complex multivariate relationships among process parameters. At the microscopic scale, static associations between nodes are quantified through discrete computation of a weight matrix, enabling the model to capture the system's short-term performance characteristics. At the macroscopic scale, a long short-term memory network models the temporal evolution of these weights, thereby capturing the long-term evolution of the system. The framework integrates multimodal data fusion and physics-informed neural network constraints to enhance generalization in small-sample scenarios. The method is empirically validated through a case study on the press-fitting process of rubber bushings into track shoes for tracked vehicles. Comparative studies show that QS-HGNN achieves higher modeling accuracy than both static and dynamic hypergraph neural networks. Finally, the model is deployed within an intelligent digital twin system for real-time press-fitting quality prediction and process control. Experimental results demonstrated a substantial improvement in quality performance: the qualification rate increased from 70% to 100%, and process stability was significantly enhanced. This research provides a high-precision, low-data-cost pathway for digital twin modeling of manufacturing process systems with progressive performance evolution, offering a scalable foundation for intelligent process optimization and quality assurance.

1. Introduction

Digital twin technology is a key enabler for manufacturing process optimization in the era of intelligent manufacturing [1,2]. A digital twin of a manufacturing process system establishes mapping relationships among process parameters, in-process states, and final product quality. An effective process model predicts product quality [3,4] before or during manufacturing, enabling timely intervention and adjustment [5,6]. This predictive capability transforms traditional manufacturing quality management from a passive "produce-then-inspect" paradigm to a proactive approach characterized by prediction, prevention, and pre-control, critical for achieving the key objectives of intelligent manufacturing [7,8].

A digital twin model of a manufacturing process system must accurately characterize both the functional behavior and performance of the system in real time—a highly challenging task [9]. The model must capture the inherent relationships among process parameters and reflect the dynamic evolution of system performance over time. During operation, various factors—such as tool or equipment wear, fixture repeatability, environmental

* Corresponding author.
E-mail address: wangjjthu@tsinghua.edu.cn (J. Wang).
[#] These authors contributed equally to this manuscript.

https://doi.org/10.1016/j.eng.2026.03.012

Please cite this article as: Y. Chen, P. Ding, J. Zhang et al., Quasi-Static Hypergraph Neural Networks: A High-Performance Approach for Digital Twin Modeling of Manufacturing Process Systems with Dynamic Performance Evolution, Engineering, https://doi.org/10.1016/j.eng.2026.03.012

conditions, and material contact properties—experience gradual or sudden changes [10–12]. Consequently, the performance of the process system evolves dynamically with accumulated operating time [13,14], exhibiting a quasi-static characteristic in which system behavior remains approximately stable in the short term while gradually changing over the long term (Fig. S1 in Appendix A). This phenomenon is observed in many manufacturing settings, with varying severity depending on the specific process. For instance, metal-cutting systems typically exhibit slower performance drift [15], whereas assembly systems involving compliant materials, such as rubber, tend to experience more rapid and significant changes. This progressive performance evolution often leads to variability in product quality, even under identical process parameter settings, posing a critical challenge for manufacturing process modeling.

Existing modeling approaches face fundamental limitations in addressing this challenge. Data-driven methods based on machine and deep learning can, in principle, approximate complex functional mappings [16,17]. However, manufacturing is a data-scarce domain, with each data point corresponding to the production of a physical product, making large-scale data collection economically impractical [18]. Hypergraph neural networks (HGNNs) offer a promising alternative by explicitly modeling multivariate associations via hypergraph structures, in which a hyperedge can connect multiple nodes simultaneously to represent the joint influence of various factors [19,20]. By embedding domain knowledge into the hypergraph topology, HGNNs can effectively reduce data dependency [21]. However, standard HGNNs assume static node relationships, failing to capture the dynamic evolution of system performance over time. Dynamic HGNNs have been developed to address this limitation by incorporating temporal modeling of graph structures [22,23]. Yet these methods require global temporal modeling of node features, graph topology, and association weights simultaneously, resulting in high model complexity and substantial data requirements [24,25]—precisely the constraints that manufacturing systems cannot satisfy.

Consequently, a gap remains: existing methods cannot effectively model the progressive performance evolution of manufacturing systems under small-sample conditions. This study proposes a quasi-static HGNN (QS-HGNN) modeling approach to address this gap. The core idea is based on a quasi-static assumption: the association strengths among process factors remain approximately constant within a single manufacturing cycle while evolving gradually across cycles, with the associations themselves remaining invariant. Thus, the manufacturing system exhibits "constant function, evolving performance,"—which translates to "fixed topology, time-varying weights" when represented via a hypergraph. The stable functional associations, grounded in domain knowledge, are encoded in the hypergraph topology; the progressive evolution of association strengths is captured by modeling the hyperedge weight matrix temporally through a long short-term memory (LSTM) network. This approach effectively captures the system's gradual time-varying characteristics under small-sample conditions. The proposed method is validated using a rubber bushing press-fitting system and deployed in a digital twin system for real-world evaluation.

The main contributions of this work are as follows:

(1) A quasi-static assumption is proposed for manufacturing process systems, revealing the inherent time-varying characteristic of "constant function, evolving performance." This assumption provides a theoretical basis for transforming the complex dynamic hypergraph modeling problem into a tractable weight matrix temporal prediction problem under fixed topology.

(2) Based on this assumption, a QS-HGNN is developed. The method encodes domain knowledge into a fixed hypergraph topology while capturing the progressive evolution of hyperedge weight matrices across cycles via an LSTM network. This approach achieves decoupled modeling of topological representation and weight evolution, effectively alleviating modeling difficulty under small-sample conditions.

(3) The practical applicability of the proposed method is validated through a rubber bushing press-fitting system and deployment in a real-world digital twin system.

(4) The remainder of this paper is organized as follows. Section 2 introduces the press-fitting case and formulates the problem. Section 3 presents the QS-HGNN methodology. Section 4 describes the experimental setup and dataset construction. Section 5 reports offline experimental results, while Section 6 demonstrates the model's deployment in a digital twin system and its real-world evaluation. Section 7 concludes the paper.

2. Application background

2.1. The rubber-bushing press-fitting process

The rubber-bushed track pin is the key connecting element in the track mechanism of tracked vehicles (Fig. 1(a)). The elastic deformation of the rubber bushing enables effective torque transmission and relative rotation of the track shoes, ensuring smooth operation of the track mechanism. Thus, the assembly quality of the rubber-bushed track pin directly affects the service life of the track mechanism and the overall reliability of the vehicle.

The assembly of the rubber bushing is known as press-fitting, in which the rubber bushing track pin is pressed into the pin ear bore of the track shoe to achieve an interference fit (Fig. 1(b)). The track pin core rod (steel 38CrSi) is pre-bonded with a rubber bushing (Shore hardness 64HA), while the pin ear bore is made of steel 42CrMo (Fig. 1(c)). The press-fitting process consists of three stages (Figs. 1(d) and (e)): (i) over-press-fitting, where the track pin is pressed beyond the designed position; (ii) back-press-fitting, where the track pin is pressed in the reverse direction for a certain distance; and (iii) settling, where the product rests for 24 h to allow stress release and deformation recovery.

The interference fit between the bushing outer diameter and the pin ear bore inner diameter demands high assembly accuracy, rubber bushing structural integrity, and sensitivity to process parameters and environmental conditions. Current practice frequently encounters issues such as inaccurate positioning and damage to bushings. Traditional parameter setting relies on operator experience and trial-and-error, and the system exhibits dynamic performance evolution characteristics, rendering fixed empirical parameters inadequate for variable production conditions. This study employs a QS-HGNN to model the press-fitting process, aiming for high-precision quality prediction and inverse optimization of process parameters.

2.2. Process quality characterization

After the settling period, the press-fit quality must be evaluated. The evaluation criteria for press-fit quality consist of two categories: assembly positional accuracy and structural integrity of the rubber bushing.

(1) Requirements for assembly positional accuracy (Fig. 1(f)): This study utilizes three key metrics to evaluate the assembly positional accuracy: Q_1: the distance L_1 from the end face of the track shoe to the end face of the track pin ((46 ± 0.5) mm) representing the track shoe position; Q_2: the distance L_2 from the end face of the rubber bushing to the end face of the track pin ((46 ± 0.5) mm) representing the bushing position; and Q_3: the distance L_3 from the end face of the rubber bushing to the end face of the track shoe, which must be less than 0, representing the overflow distance.

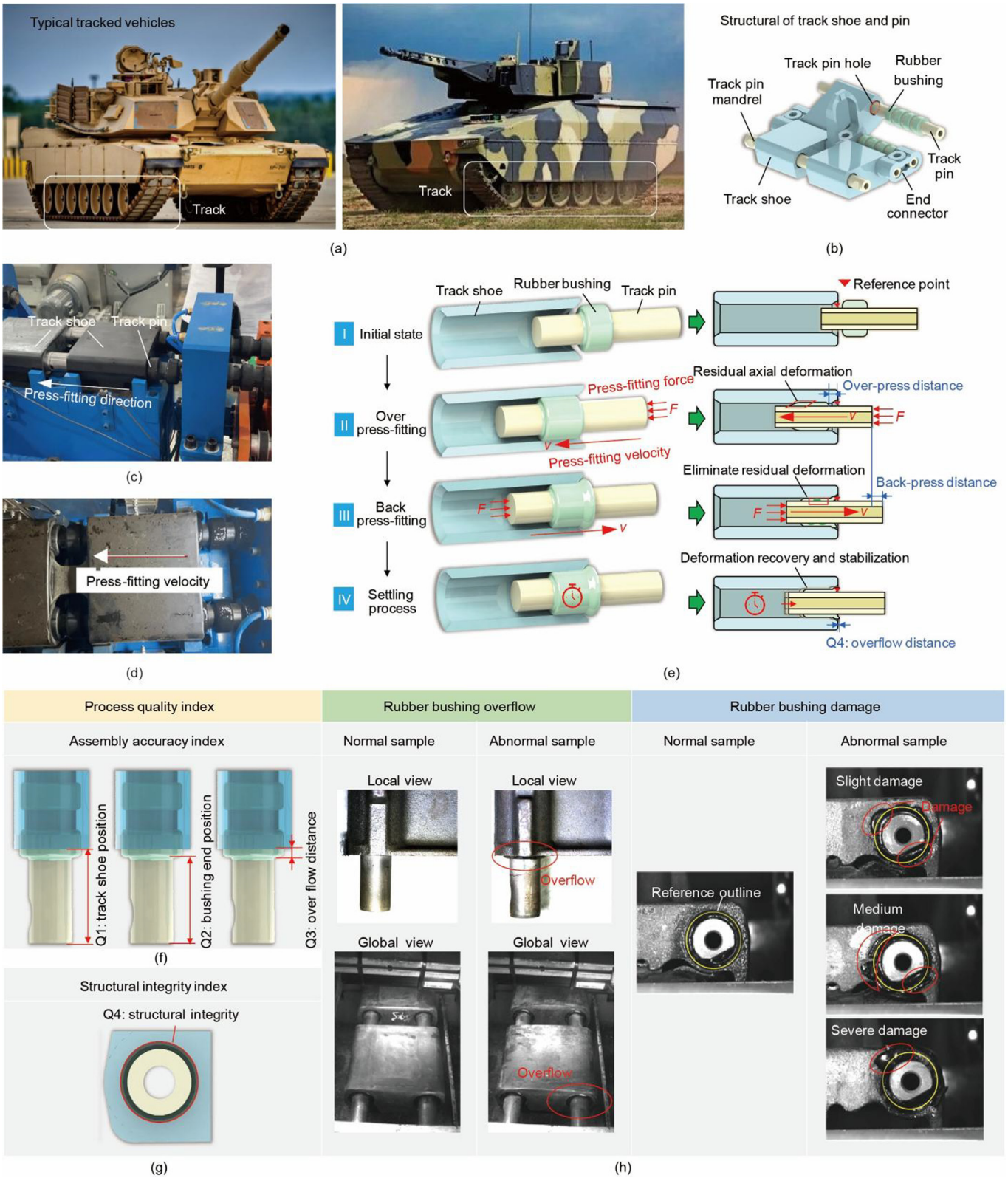

Fig. 1. The rubber bushing press-fitting process for the track shoe: (a, b) structural composition of the track; (b) structural composition of the track shoe and pin; (c, d) physical images of the press-fitting process; (e) press-fitting procedure: over-press-fitting, back-press-fitting, and settling, along with the main process parameters: over-press distance and back-press distance, press-fitting force (F), press-fitting velocity (v); (f) position accuracy quality indicators: Q_1, Q_2, and Q_3; (g) bushing structural integrity quality indicator: Q_4; and (h) typical defective products.

These three metrics satisfy a definite geometric relationship, expressed as:

$$L_3 = L_1 - L_2 \tag{1}$$

Excessively large or small measurements can lead to "overflow" in the rubber bushing, preventing installation of the end connector and causing localized stress concentration on the end face during service, thereby compromising service life.

(2) Structural integrity of the rubber bushing (Fig. 1(g)) is affected during press-fitting due to significant interference between the track pin and pin hole, resulting in substantial radial compressive stress on the rubber bushing. This stress can lead to peeling or damage to the rubber from the track pin. Bushing damage manifests in two forms: one occurs inside the pin hole, characterized by internal tearing of the rubber material, which can be detected by evaluating the bushing position; the other occurs at the outer edge of the pin hole, causing abnormal rubber bulging (Fig. 1(h)). These edge bulges create stress concentration points that may propagate during tracked vehicle operation, significantly reducing the bushing's service life. Q_4 denotes the structural integrity of the rubber bushing.

2.3. Factors affecting press-fitting quality

Based on existing issues in the press-fitting process, preliminary observations, and statistical analysis, the main factors affecting press-fitting quality can be summarized into three categories: geometric dimensions, process parameters, and environmental factors.

(1) Material geometric dimensions: The shaft diameter of the track pin and the bore diameter of the pin hole are critical, as they determine the interference fit.

(2) Press-fitting process parameters: Over-press distance, back-press distance, and press-fitting velocity are crucial. The displacement controls the final position of the track pin, while the velocity affects the stress state of the rubber bushing during assembly.

(3) Environmental factors: Temperature is the primary factor, fluctuating between −5 and 35 °C in practical workshops. Due to rubber's high sensitivity of rubber's mechanical properties to temperature, the deformation behavior and stress distribution of the rubber bushing are significantly affected.

(4) Uncertainties in the press-fitting process: Press-fitting quality is also influenced by factors that are difficult to measure or quantify, such as the real-time state of the press machine and the dynamic friction coefficient between the bushing and pin hole. These uncertainties cause variations in assembly quality under the same process parameters (Fig. S2(a) in Appendix A). Although these factors cannot be measured directly, their effects are reflected in the dynamic process data (Fig. S2(b) in Appendix A).

In summary, when modeling the press-fitting process of the rubber bushing, it is essential to consider the influence of geometric dimensions, process parameters, and environmental factors on assembly quality, as well as the impact of uncertainties manifested in the dynamic process data (Fig. S2(c) in Appendix A).

3. Principles of quasi-static hypergraph network

3.1. Quasi-static assumption

In many manufacturing process systems, system performance evolves dynamically due to the coupling of internal and external factors, leading to shifts in the mapping between process parameters and assembly quality. The variation is often subtle within a single manufacturing run but accumulates over extended operation, manifesting as continuous performance adjustments. These characteristics can be described as quasi-static: at shorter time scales, the system appears to be in a steady state or static, while at longer time scales, it exhibits dynamic changes. Within a quasi-static system, performance evolution leads to changes in the mapping between process parameters and assembly quality, primarily reflected in stable association relationships with varying strengths. When modeling with a hypergraph network structure, this corresponds to an invariant hypergraph topology with dynamically adjusted hyperedge weights, represented through temporal variations in the weight matrix.

Based on this assumption, the following sections present the proposed QS-HGNN, which fixes the hypergraph topology to encode domain knowledge while modeling the temporal evolution of hyperedge weights to capture progressive performance changes. A detailed comparison with static and dynamic hypergraph methods is provided in Section 3.6.

3.2. Network architecture

Based on the quasi-static assumption of manufacturing process system performance evolution, this study proposes a QS-HGNN that constructs the model from a quasi-static perspective: at the microscopic time scale, the system is treated as static with stable hypergraph topology and association strengths; at the macroscopic time scale, the focus shifts to capturing the gradual evolution of these association strengths.

In the QS-HGNN, each manufacturing process step is treated as a fundamental sampling unit, discretizing continuous temporal evolution into a series of static snapshots. At each discrete time point, graph convolution operations solve for the weight matrix, quantifying the mapping relationship between process parameters and quality and distinguishing time-varying from time-invariant factors. Based on the obtained discrete temporal sequence of weight matrices, a progressive evolutionary temporal model captures the long-term trend in system variation. This design achieves dual representation of system characteristics: at the microscopic level, graph convolution inversion at a single time point captures the instantaneous static properties of the system, that is, the instantaneous mapping between process parameters and quality; at the macroscopic level, the temporal evolution of the weight matrix corresponds to the system's gradual evolution over extended time scales. This multi-time-scale decoupled modeling approach accurately characterizes the influence mechanisms between process parameters and press-fitting quality and captures the temporal evolution trends of these influence relationships. The detailed network architecture is illustrated in Fig. 2.

3.3. Weight matrix estimation

In each manufacturing process, estimating the hypergraph weight matrix that represents the strength of associations among process parameters, variables, and quality is crucial for constructing the QS-HGNN. The following presents the derivation of the weight matrix calculation.

Each manufacturing process step is considered an instance, arranged sequentially to form a discrete time series, represented as a set of heterogeneous hypergraphs over time:

$$G = \{G_t \mid t \in T\} \tag{2}$$

where T denotes the set of discrete time points, with t representing each time point. G represents the complete hypergraph collection, and each G_t represents a hypergraph instance constructed from press-fitting data at time t. The definition of G_t is as follows:

$$G_t = (V_t, \varepsilon_t, \boldsymbol{W}_t) \tag{3}$$

where V_t denotes the set of nodes, ε_t represents the set of hyperedges, and $\boldsymbol{W}_t$ is the weight matrix. $|V_t|$ indicates the number of

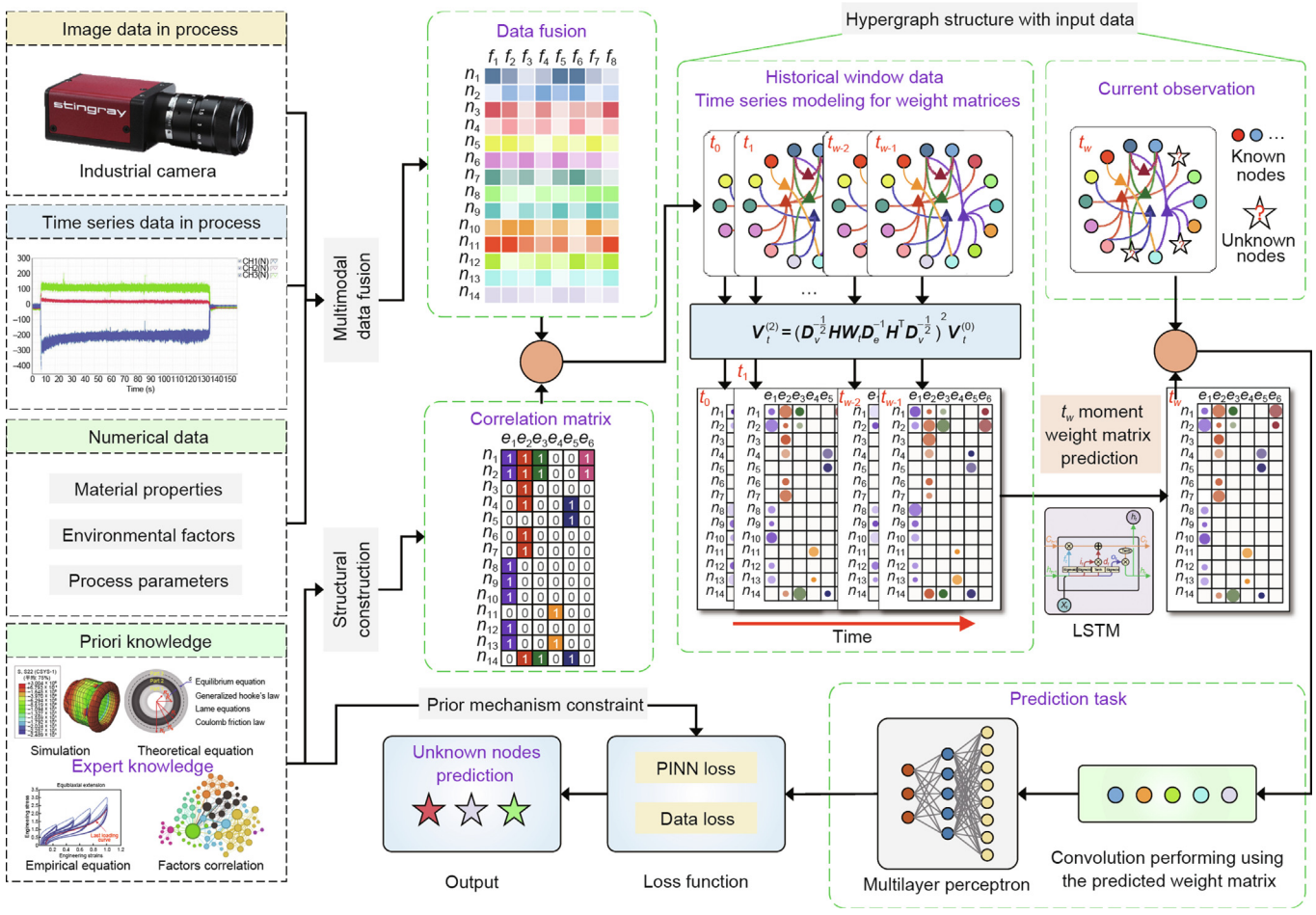

Fig. 2. QS-HGNN architecture.

nodes, and $|\varepsilon_t|$ denotes the number of hyperedges. The incidence matrix $\boldsymbol{H}\in\mathbb{R}^{|Vt|\times|\varepsilon t|}$ represents the connectivity between neighborhoods:

$$\boldsymbol{H}(v,e)=\begin{cases}1, & \text{when} \quad v\in e\\ 0, & \text{when} \quad v\notin e\end{cases} \tag{4}$$

where $v\in e$ indicates that node v is connected through hyperedge e. The incidence matrix captures the topology of the hypergraph. In this study, the topology is determined based on expert knowledge of the manufacturing process.

In feature learning tasks with hypergraph structures, convolution operations extract local node information. A single-layer hypergraph convolutional network captures node features within the first-order neighborhood—information from nodes directly connected to the target node. In contrast, a two-layer hypergraph convolutional network captures node features within the second-order neighborhood, including information from the neighbors of the target node's neighbors. This study employs a two-layer hypergraph convolutional neural network to obtain node feature representations.

For each manufacturing step, the spatial domain hypergraph convolution models higher-order relationships through a two-step information propagation mechanism: the first step involves feature propagation from nodes to hyperedges, with each hyperedge aggregating features from all connected nodes to obtain its representation; the second step involves aggregation from hyperedges back to nodes, where each node updates its representation by aggregating features from the hyperedges to which it belongs. Thus, the spatial domain hypergraph convolution can be defined as follows:

$$\begin{cases}\boldsymbol{m}_{e,t}^{(l)}=\sum_{v\in N_v(e)}M_v^{(l)}\left(\boldsymbol{x}_{v,t}^{(l)}\right)\\ \boldsymbol{y}_{e,t}^{(l)}=U_e^{(l)}\left(W_{e,t},\boldsymbol{m}_{e,t}^{(l)}\right)\end{cases}\quad\text{Step 1}$$

$$\begin{cases}\boldsymbol{m}_{v,t}^{(l+1)}=\sum_{e\in N_e(v)}M_e^{(l)}\left(\boldsymbol{x}_{v,t}^{(l)},\boldsymbol{y}_{e,t}^{(l)}\right)\\ \boldsymbol{x}_{v,t}^{(l+1)}=U_v^{(l)}\left(\boldsymbol{x}_{v,t}^{(l)},\boldsymbol{m}_{v,t}^{(l+1)}\right)\end{cases}\quad\text{Step 2} \tag{5}$$

Here, $N_v(e)$ denotes the node neighborhood set of hyperedge e. Similarly, and $N_e(v)$ denotes the hyperedge neighborhood set of node v. The topological information of these graphs remains constant over time. The subscript t distinguishes values that vary at different time points $\boldsymbol{x}_{v,t}^{(l)}$ is the feature of node v at layer l and time t, $\boldsymbol{m}_{e,t}^{(l)}$ is the aggregated message from all nodes connected to hyperedge e, $W_{e,t}$ is the hyperedge weight, and $\boldsymbol{y}_{e,t}^{(l)}$ is the updated hyperedge feature. $\boldsymbol{m}_{v,t}^{(l+1)}$ is the message passed back to node v, and $\boldsymbol{x}_{v,t}^{(l+1)}$ is the updated node feature. The two-step message-passing process operates as follows: Step 1 aggregates node features into hyperedge representations via the node message function $M_v^{(l)}$ and the hyperedge update function $U_e^{(l)}$; Step 2 propagates hyperedge information back to nodes via the hyperedge message function $M_e^{(l)}$ and the node update function $U_v^{(l)}$.

The four message and update functions are defined as normalization and weighted aggregation operations. The function $\sigma(\cdot)$

denotes a nonlinear activation function. Using the incidence matrix $\boldsymbol{H}$ of the hypergraph, along with the node degree matrix $\boldsymbol{D}_v$ and the hyperedge degree matrix $\boldsymbol{D}_e$:

$$\begin{cases} \boldsymbol{D}_v = \mathrm{diag}\left(\sum_{j=1}^{|\varepsilon|} \boldsymbol{H}(i,j)\right), & i = 1,2,...,|V| \\ \boldsymbol{D}_e = \mathrm{diag}\left(\sum_{i=1}^{|V|} \boldsymbol{H}(i,j)\right), & j = 1,2,...,|\varepsilon| \end{cases} \tag{6}$$

Let $\boldsymbol{V}_t^{(l)}$ denote the node feature matrix at time t and layer l, the two-step hypergraph convolution at layer $l+1$ can be expressed in matrix form as:

$$\boldsymbol{V}_t^{(l+1)} = \sigma\left(\boldsymbol{D}_v^{-\frac{1}{2}}\boldsymbol{H}\boldsymbol{W}_t\boldsymbol{D}_e^{-1}\boldsymbol{H}^{\mathrm{T}}\boldsymbol{D}_v^{-\frac{1}{2}}\boldsymbol{V}_t^{(l)}\right) \tag{7}$$

where symmetric two-sided normalization is adopted to enhance the model's stability and numerical representation capability.

In subsequent computations, the activation function within the hypergraph convolution layers is removed. This decision is based on the observation that the commonly used Rectified Linear Unit (ReLU) activation function in mainstream hypergraph convolutional networks behaves as a linear function in the positive domain. Additionally, this study retains nonlinear activation functions in downstream tasks, where nonlinear transformations effectively capture the data's features. Therefore, adding activation functions within the convolutional layers increases computational overhead and may introduce redundant nonlinear transformations. This simplification maintains the model's representational capacity while enhancing computational efficiency. The simplified formulation is expressed as:

$$\boldsymbol{V}_t^{(2)} = \boldsymbol{D}_v^{-\frac{1}{2}}\boldsymbol{H}\boldsymbol{W}_t\boldsymbol{D}_e^{-1}\boldsymbol{H}^{\mathrm{T}}\boldsymbol{D}_v^{-\frac{1}{2}}\boldsymbol{D}_v^{-\frac{1}{2}}\boldsymbol{H}\boldsymbol{W}_t\boldsymbol{D}_e^{-1}\boldsymbol{H}^{\mathrm{T}}\boldsymbol{D}_v^{-\frac{1}{2}}\boldsymbol{V}_t^{(0)} \tag{8}$$

where, both $\boldsymbol{D}_v$ and $\boldsymbol{D}_e$ are diagonal matrices, defined as follows:

$$\widetilde{\boldsymbol{H}} = \boldsymbol{D}_v^{-\frac{1}{2}}\boldsymbol{H}, \widetilde{\boldsymbol{W}} = \boldsymbol{W}_t\boldsymbol{D}_e^{-1}, \widetilde{\boldsymbol{H}}^{\mathrm{T}} = \boldsymbol{H}^{\mathrm{T}}\boldsymbol{D}_v^{-\frac{1}{2}} \tag{9}$$

Eq. (8) can then be expressed as:

$$\boldsymbol{V}_t^{(2)} = \widetilde{\boldsymbol{H}}\widetilde{\boldsymbol{W}}\widetilde{\boldsymbol{H}}^{\mathrm{T}}\widetilde{\boldsymbol{H}}\widetilde{\boldsymbol{W}}\widetilde{\boldsymbol{H}}^{\mathrm{T}}\boldsymbol{V}_t^{(0)} \tag{10}$$

Define the transformation matrix ($\boldsymbol{Q}$) as:

$$\boldsymbol{Q} = \widetilde{\boldsymbol{H}}\widetilde{\boldsymbol{W}}\widetilde{\boldsymbol{H}}^{\mathrm{T}} \tag{11}$$

Then, the convolution formula can be expressed as:

$$\boldsymbol{V}_t^{(2)} = \boldsymbol{Q}^2\boldsymbol{V}_t^{(0)} \tag{12}$$

Each manufacturing instance is treated as an independent hypergraph. In this hypergraph, the formation of process quality closely parallels the information aggregation mechanism in hypergraph convolution; the quality is influenced by process parameters and process variables, similar to how a target node updates its representation by aggregating information from its neighborhood in hypergraph convolution. Based on this isomorphism, process parameters and process variables serve as the initial feature values of the input nodes, while quality indicators correspond to the feature values of the target nodes after two layers of hypergraph convolution-based information aggregation. This modeling approach aligns with the physical essence of information flow and influence transmission in manufacturing processes, where the input nodes comprise n_1 nodes representing process parameters and process variables, and the target nodes include n_2 nodes related to quality indicators. The initial feature values of the target nodes are set to 0.

For computational convenience, the feature values of the process parameter and process variable nodes are defined as the first n_1 rows of the graph-structured data $\boldsymbol{V}_t$, while the target nodes occupy the last n_2 rows. The index set of the last n_2 rows is denoted as $\boldsymbol{S}$. Thus:

$$\boldsymbol{V}_t^{(2)}[\boldsymbol{S},:] = \left(\boldsymbol{Q}^2\right)[\boldsymbol{S},:]\boldsymbol{V}_t^{(0)} \tag{13}$$

The solution is obtained using the Moore–Penrose pseudoinverse:

$$\left(\boldsymbol{Q}^2\right)[\boldsymbol{S},:] = \boldsymbol{V}_t^{(2)}[\boldsymbol{S},:]\boldsymbol{V}_t^{(0)^+} \tag{14}$$

To simplify the calculation, define $\boldsymbol{Q}_{\mathrm{partial}}$ as:

$$\boldsymbol{Q}_{\mathrm{partial}}^2 = \left(\boldsymbol{Q}^2\right)[\boldsymbol{S},:] \tag{15}$$

Therefore, the weight matrix at time t is obtained as:

$$\boldsymbol{W}_t = \widetilde{\boldsymbol{W}}\boldsymbol{D}_e^{\frac{1}{2}} = \widetilde{\boldsymbol{H}}_{\mathrm{partial}}^{+}\,\boldsymbol{Q}_{\mathrm{partial}}\,\boldsymbol{H}^{\mathrm{T}^+}\boldsymbol{D}_e^{\frac{1}{2}} \tag{16}$$

where $\boldsymbol{H}\sim_{\mathrm{partial}} = \boldsymbol{H}\sim[\boldsymbol{S},:]$. The weight matrix $\boldsymbol{W}_t$ describes the coupling strength between process parameters, process variables, and quality indicators at time t. Through graph convolution-based discrete solving, the collection of weight matrices $\boldsymbol{W}$ reflecting the system at each time point is obtained:

$$\boldsymbol{W} = \{\boldsymbol{W}_t \mid t \in T\} \tag{17}$$

3.4. Time series modeling

Time series modeling is conducted using the weight matrices to characterize the progressive evolution of the interaction strengths among various elements in the press-fit assembly system. Specifically, a historical window of size w is defined, and the weight matrices in the sliding time window $\{\boldsymbol{W}_{t-w}, \ldots, \boldsymbol{W}_{t-1}\}$ are used to predict the weight matrix at the next time point, $\boldsymbol{W}_t$. Here, an LSTM model is employed to model the historical data:

$$\hat{\boldsymbol{W}}_t = f_{\mathrm{LSTM}}(\boldsymbol{W}_{t-w}, ..., \boldsymbol{W}_{t-1}) \tag{18}$$

where f_{LSTM} represents the LSTM network, and $\hat{\boldsymbol{W}}_t$ denotes the predicted weight matrix at time t.

Next, combining the initial node features $\boldsymbol{x}_t$ at time t and the hypergraph incidence matrix $\boldsymbol{H}$, the assembly quality ($\hat{y}_t$) at time t is predicted using hypergraph convolution, expressed as:

$$\begin{aligned} \boldsymbol{y}_t^{(1)} &= \sigma\left(\boldsymbol{D}_v^{-\frac{1}{2}}\boldsymbol{H}\hat{\boldsymbol{W}}_t\boldsymbol{D}_e^{-1}\boldsymbol{H}^{\mathrm{T}}\boldsymbol{D}_v^{-\frac{1}{2}}\boldsymbol{x}_t^{(0)}\Theta\right) \\ \hat{\boldsymbol{y}}_t &= \sigma\left(\boldsymbol{D}_v^{-\frac{1}{2}}\boldsymbol{H}\hat{\boldsymbol{W}}_t\boldsymbol{D}_e^{-1}\boldsymbol{H}^{\mathrm{T}}\boldsymbol{D}_v^{-\frac{1}{2}}\boldsymbol{y}_t^{(1)}\Theta\right) \end{aligned} \tag{19}$$

where Θ represents the parameters to be learned by the model. The model is optimized by minimizing the deviation between the predicted values $\hat{y}$ and the true assembly quality indicators y. The loss function ($\mathscr{L}_G$) is defined as:

$$\mathscr{L}_G = \frac{1}{N}\sum_{i=1}^{N}\left(\hat{y}_i - y_i\right)^2 \tag{20}$$

where $\hat{y}_i$ is the predicted value of the model, y_i is the experimentally obtained true value, and N is the total number of samples.

By leveraging physics-informed neural networks (PINNs), the QS-HGNN incorporates physical constraints. By embedding mechanistic relationships among manufacturing process parameters, process variables, and process quality into the modeling process, this framework integrates data-driven predictions of quality indicators with physical models and constraints to refine predictions. The physical constraints used in this study derive from our previous research on the mechanical analysis of the press-fitting process [26,27]. A cascaded ultitask physics-informed neural network (CM-PINN) loss term ($\mathscr{L}_{\mathrm{PINN}}$) is defined as follows:

$$\mathscr{L}_{\mathrm{PINN}} = \frac{1}{N}\sum_{i=1}^{N}\left(\hat{y}_{\mathrm{damage},i} - y_{\mathrm{damage},i}^{\mathrm{PINN}}\right)^2 \tag{21}$$

where $\hat{y}_{\text{damage},i}$ is the predicted quality value by the model and $y^{\text{PINN}}_{\text{damage},i}$ is the predicted value calculated based on the mechanistic relationships. The final total loss function is expressed as:

$$\mathscr{L} = \alpha \mathscr{L}_G + \beta \mathscr{L}_{\text{CM-PINN}} \tag{22}$$

where α and β are hyperparameters that balance the importance of each loss component. The hypergraph loss term $\mathscr{L}_G$ captures implicit, experience-driven patterns from industrial data, while the physics-informed loss term $\mathscr{L}_{\text{CM-PINN}}$ ensures basic physical consistency derived from mechanistic analysis. Recent studies have explored embedding physical structures directly into neural network architectures for intelligent manufacturing, providing valuable insights and representing a promising direction for future work [28,29].

Compared with traditional HGNNs, which require learning the weight matrix during training, the QS-HGNN directly obtains it from discretized solutions. This design restricts the model's trainable parameters to three components: the LSTM model parameters for time-series evolution (Eq. (18)), the hypergraph convolution parameters at time t (Eq. (19)), and the weighting coefficients in the loss function (Eq. (21)). This structure enables effective learning under small-sample conditions, addressing the high sample acquisition costs in industrial scenarios.

3.5. Construction of the press-fitting system graph structure

Based on the actual scenario of rubber bushing press-fitting, this study constructs a hypergraph with 12 nodes (n_1–n_{12}) and 4 hyperedges (e_1–e_4) to represent the relationships among various factors during the press-fitting process. The force sequence node is represented by temporal features extracted via an LSTM network; the image node by visual features extracted via a pre-trained convolutional neural network (VGG16); and the other numerical feature nodes are standardized and normalized (Fig. 3(a)).

The design of the four hyperedges is based on the physical mechanisms of the rubber bushing press-fitting process and engineering domain knowledge, validated through data correlation analysis (Table 1).

The engineering significance of the hyperedge structure lies in its ability to encode relationships between influencing factors and quality outcomes, clearly expressing which factors affect assembly quality and how they are coupled (Fig. 3(b)). Hyperedge e_1 connects process parameters (press-fitting date, environmental temperature, press-fitting velocity, bushing shaft diameter, and inner hole diameter) with observation data nodes (force–displacement curves and press-fitting images), indicating that process parameters collectively impact observation data, which also complement each other. As detailed in Section 4.1, force–displacement curves reflect factors that are difficult to measure directly (e.g., instantaneous friction changes), while image data captures deformation states and surface lubrication conditions. Hyperedge e_2 connects environmental temperature, bushing shaft diameter, inner hole diameter, and damage status nodes, highlighting that geometric dimensions and environmental temperature are key factors influencing the structural integrity of the bushing. The correlation analysis in Table 1 shows that the bushing shaft diameter has the highest correlation coefficient (0.317) with structural damage among all process parameters, supporting this design. Hyperedge e_3 connects force–displacement curves, press-fitting images, and damage status nodes, as process variables are also important references for detecting press-fitting abnormalities in addition to preset process parameters. Hyperedge e_4 connects force–displacement curves, press-fitting images, over-press distance, back-press distance, overflow distance, and track shoe position nodes, since press-fitting quality evaluation metrics relate to both process variables and final-stage process parameters, with intrinsic correlations among these evaluation indicators. This is confirmed by Table 1, where over-press and back-press distances show strong correlations with overflow distance (0.586 and 0.594, respectively). This physics-informed hyperedge design effectively embeds domain knowledge into the graph structure.

3.6. Principle comparison with static and dynamic hypergraphs

Existing HGNN methods have limitations in handling quasi-static problems because they fail to capture unique characteristics. Static HGNNs (Fig. 4(a)) use fixed hypergraph structures and weights, assuming system properties remain constant, which prevents them from characterizing long-term progressive evolution. Dynamic HGNNs (Fig. 4(b)) introduce temporal modeling mechanisms to capture dynamic changes but require large amounts of training data. Their training involves global-temporal modeling of node features, hypergraph structures, and associated weights simultaneously, resulting in low utilization of domain knowledge. This includes time-invariant node data and time-variant hyperedge data in the temporal analysis framework, obscuring true evolutionary patterns and preventing the model from focusing on the progressive variation in relationship strengths, thereby leading to high training costs.

The QS-HGNN, based on the quasi-static assumption, performs temporal modeling only on the weight matrices (Fig. 4(c)) while keeping the graph topology stable. This design captures the progressive evolution characteristics of relationship strengths within the manufacturing system and significantly reduces parameter complexity. It achieves an optimal balance between modeling accuracy and computational efficiency under small-sample conditions, making it well-suited to the inherent nature of manufacturing process systems where functions remain relatively stable while performance changes dynamically.

4. Experimental system and data preparation

4.1. Intelligent press-fitting system setup

As discussed in Section 2.3, uncertainty factors in the press-fitting process are reflected in the dynamic response data. Active data collection included conventional force–displacement curves and images captured throughout the press-fitting operation to gather richer process information. This approach provides a process modeling method that integrates static process parameters with dynamic process data.

The force–displacement curve is a critical dynamic parameter during the press-fitting process (Fig. 5), recording the real-time variation in force and displacement. It reflects material deformation, stress changes, and potential defect formation. Each curve represents a complete press-fitting cycle. Differences among curves obtained under identical process parameters can indicate hard-to-measure factors, such as instantaneous changes in friction coefficients or transient states of the press-fitting equipment.

Image data, another key information source, visually captures geometric shape changes, surface features, and potential anomalies during the press-fitting operation. Images taken during the process, particularly those capturing the rubber press-fitting into the pin hole, provide two key types of visual information, Fig. 5(d):

(1) Deformation state analysis: Under normal conditions, the rubber bushing should show a symmetrical deformation pattern. Fig. 5(d) highlights abnormalities, including localized protrusions (yellow circle) and abnormally narrow gaps between adjacent bushings (red circle), which indicate potential assembly issues.

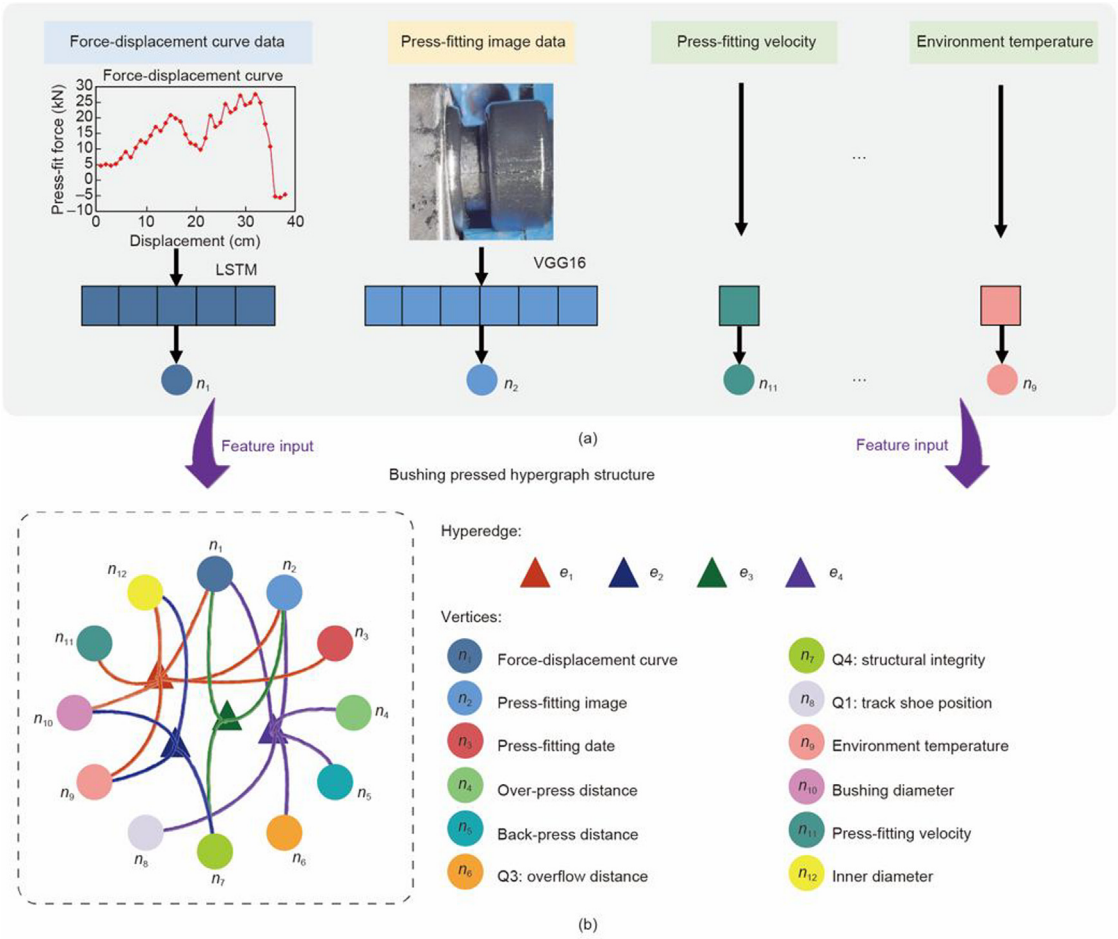

Fig. 3. Hypergraph structure of the rubber bushing press-fitting process model: (a) meaning of the nodes; and (b) hypergraph representation of the press-fitting process model.

Table 1
Correlation analysis between process parameters and quality indicators.

Process parameters	Overflow distance	Track shoe position	Structural integrity
Environment temperature	–0.165	0.265	0.079
Press-fitting velocity	0.434	–0.290	0.041
Over-press distance	0.586	0.355	0.050
Back-press distance	0.594	0.134	0.038
Bushing shaft diameter	0.185	–0.026	0.317

(2) Surface lubrication condition assessment: The surface reflectivity characteristics of the rubber bushing serve as a crucial indicator for evaluating lubrication conditions. In Fig. 5(d), a well-lubricated bushing exhibits uniform surface gloss, whereas insufficient lubrication results in reduced gloss and localized dark areas, indicating a risk of excessive friction during press-fitting.

4.2. Dataset construction

Prior to dataset construction, three types of raw data are preprocessed: force–displacement curves are encoded using an LSTM network, images are processed via a VGG16-based transfer learning pipeline, and numerical parameters are standardized using Z-score normalization (details in Section S1 (data preprocessing) in Appendix A).

Historical data embodies inherent patterns of system performance evolution. To effectively utilize this historical data and capture the progressive evolution characteristics of the press-fitting system, this study employs a sliding time window method to construct the dataset, combining features from multiple consecutive press-fitting cycles into a single sample. Each press-fitting cycle is assigned a standardized timestamp by calculating the time difference relative to a reference time (T_i):

$$T_i = \frac{C_i - C_0}{\Delta t} \tag{23}$$

where C_i is the sampling time, C_0 is the selected reference time, and Δt is the time unit (e.g., day, hour, or minute).

The time series dataset is constructed using a sliding time window Fig. 6(a). For a fixed window size w and prediction time t_n, the input to the prediction model consists of two parts: historical press-fitting data from t_{n-w} to t_{n-1}, to capture the long-term evolutionary trend of the system, and the process parameters and data at time t_n, to obtain the real-time state of the current manufacturing process. The model's prediction target is the process quality at time t_n. This construction integrates the system's long-term evolutionary trend with its instantaneous state (Figs. 6(b) and (c)), and enables data augmentation by varying the window size.

The dataset was collected from an industrial press-fitting production line from September 21, 2023, to June 13, 2024, covering approximately 10 months of operations. A total of 200 press-fitting cycles were recorded, following the factory's production schedule, resulting in a non-uniform distribution over time. Each timestamp corresponds to one complete press-fitting cycle, which includes the sequential pressing of eight bushings. After applying

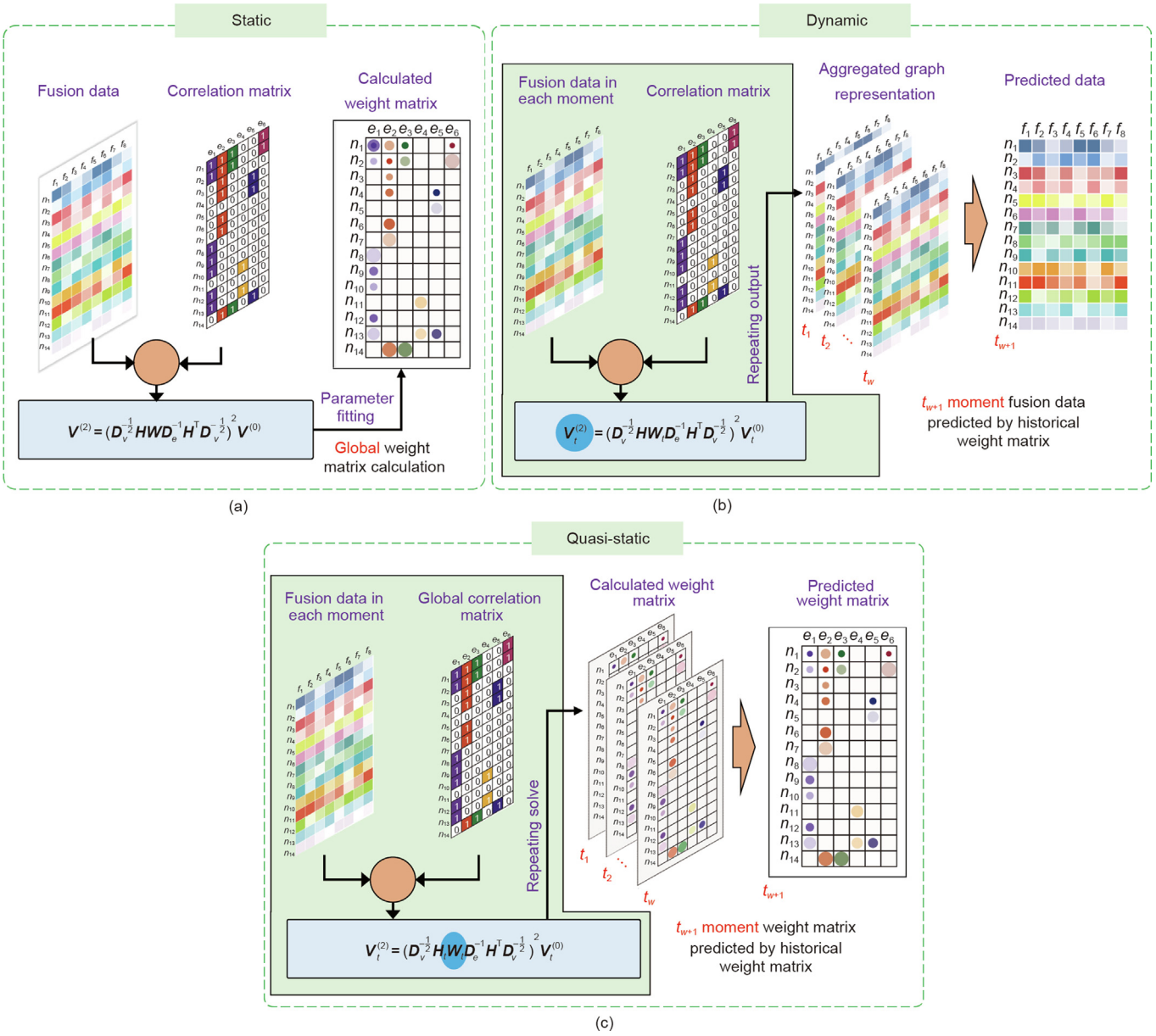

Fig. 4. Comparison of the three types of hypergraph networks: (a) static hypergraph; (b) dynamic hypergraph; and (c) quasi-static hypergraph.

the sliding time window strategy with w = 30, 170 samples were generated for model training and evaluation. The selection of w = 30 balances the capture of sufficient evolutionary patterns with the need for adequate training samples; corresponding sensitivity analysis is provided in Section S2 in Appendix A. During each press-fitting cycle, the force–displacement signal was sampled at 0.5 s intervals, and the press-fitting velocity varied from 8 to 25 mm·s^{-1} to cover diverse conditions.

5. Offline evaluation of model's performance

In this section, the proposed model's performance and advantages are validated using the press-fit manufacturing process of the track shoe, a key component of tracked vehicles, as a case study.

Offline experiments were conducted using 170 samples constructed in Section 4.2. Each sample contains multi-dimensional information, including force–displacement curve data, press-fitting process images, environmental temperature, shaft diameter, press-fitting velocity, over-press distance, back-press distance, damage status, rubber bushing overflow distance, and track shoe position. The data was split into training and testing sets at an 80:20 ratio.

The QS-HGNN model was implemented in Python 3.8.0 and PyTorch 1.13.1, and trained on a server equipped with an NVIDIA RTX 4090 GPU (NVIDIA Corporation, USA) and 80 GB of memory. The Tanh activation function, Xavier initialization, and Adam optimizer (learning rate = 0.001) were used for training.

5.1. Model validation and analysis based on comparative experiments

Based on the trained models, predictions and analyses were conducted on three key indicators of assembly quality. As shown in Fig. 7, the QS-HGNN demonstrates strong accuracy and consistency across multiple prediction tasks. For the regression predictions of the track shoe position (Fig. 7(b-i)) and the overflow

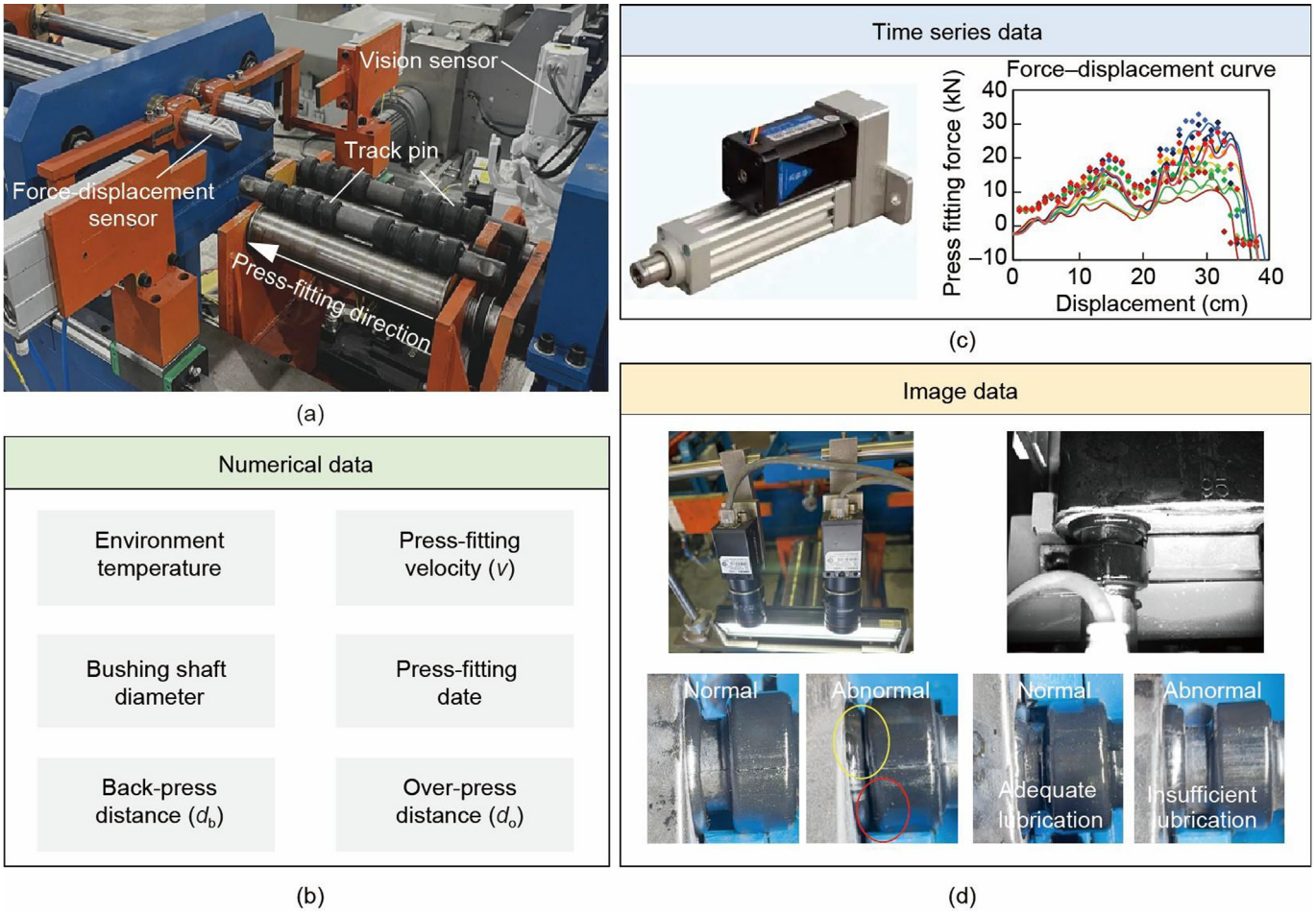

Fig. 5. Construction of the intelligent press-fitting system: (a) system hardware; (b) controllable influencing factors and process parameters that can be collected; (c) force–displacement curves collected during the press-fitting process; and (d) image data of the rubber bushing captured during the press-fitting process.

distance (Fig. 7(b-ii)), the predicted values closely align with the actual values, with coefficient of determination R^2 values of 84.64% and 85.2%, respectively. In the classification task for structural integrity prediction (Fig. 7(b-iii)), the model achieved 100% accuracy in distinguishing between "intact" and "damaged" states, correctly identifying all 25 intact samples and 10 damaged samples. This high accuracy is mainly attributed to the introduction of the physics-informed CM-PINN loss constraint, which significantly enhanced the model's classification capability for structural integrity, further validating the importance of incorporating physical constraints to improve model performance.

To demonstrate the superiority of the proposed model, it was compared with static and dynamic HGNNs under the same limited-data industrial setting. For the static HGNN, the prediction of unknown nodes is completed by randomly initializing the weight matrix and optimizing it during training, as shown in Fig. 7(c). In the dynamic HGNN, after aggregating and updating node features, the entire graph is temporally modeled to predict the unknown nodes at the current time, as illustrated in Fig. 7(d). Experimental results indicate that the static HGNN yields the lowest R^2 values (36.7% for track shoe position, 46.97% for overflow distance) due to its fixed weight matrix, which cannot account for the progressive performance evolution observed in the 10-month production dataset. The dynamic HGNN achieves moderate R^2 values (61.94% and 31.12%) but exhibits unstable predictions, particularly for overflow distance. Its global temporal modeling of all node features and graph structures requires more parameters than the 170 samples can effectively support. In contrast, the QS-HGNN achieves the highest prediction accuracy (84.64% and 85.2%) with 100% structural integrity classification. Its compact structure—fixing the topology while modeling the evolution of the weight matrix—aligns with the quasi-static nature of the press-fitting system and maintains a manageable parameter space with limited data.

To further compare the performance of these three networks, an analysis of their loss function training curves (Fig. 8) reveals that the dynamic HGNN exhibits significant fluctuations during training, with large and unstable loss value oscillations. The static HGNN shows a relatively smooth decline in loss, but the final converged loss value is high, suggesting limited fitting capability. In contrast, the QS-HGNN maintains a stable training process while achieving a lower final loss value, indicating good convergence performance. The R^2 trends corroborate these findings: the dynamic hypergraph's R^2 fluctuates dramatically despite high peaks; the static hypergraph's R^2 remains stable but low; the QS-HGNN's R^2 rises steadily to a high level with consistent stability.

In addition to the comparative experiments, ablation studies were conducted to evaluate the necessity of different components in QS-HGNN (detailed results in Section S3 in Appendix A). Selectively removing multimodal inputs and the CM-PINN constraint confirmed that force–displacement curve features, image features, and the physics-informed constraint all significantly contribute to prediction accuracy—in particular, removing the CM-PINN constraint caused pronounced degradation in track shoe position and bushing end-face position predictions. Further experiments targeting the hypergraph structure—removing hyperedge e_3, adding a fully connected

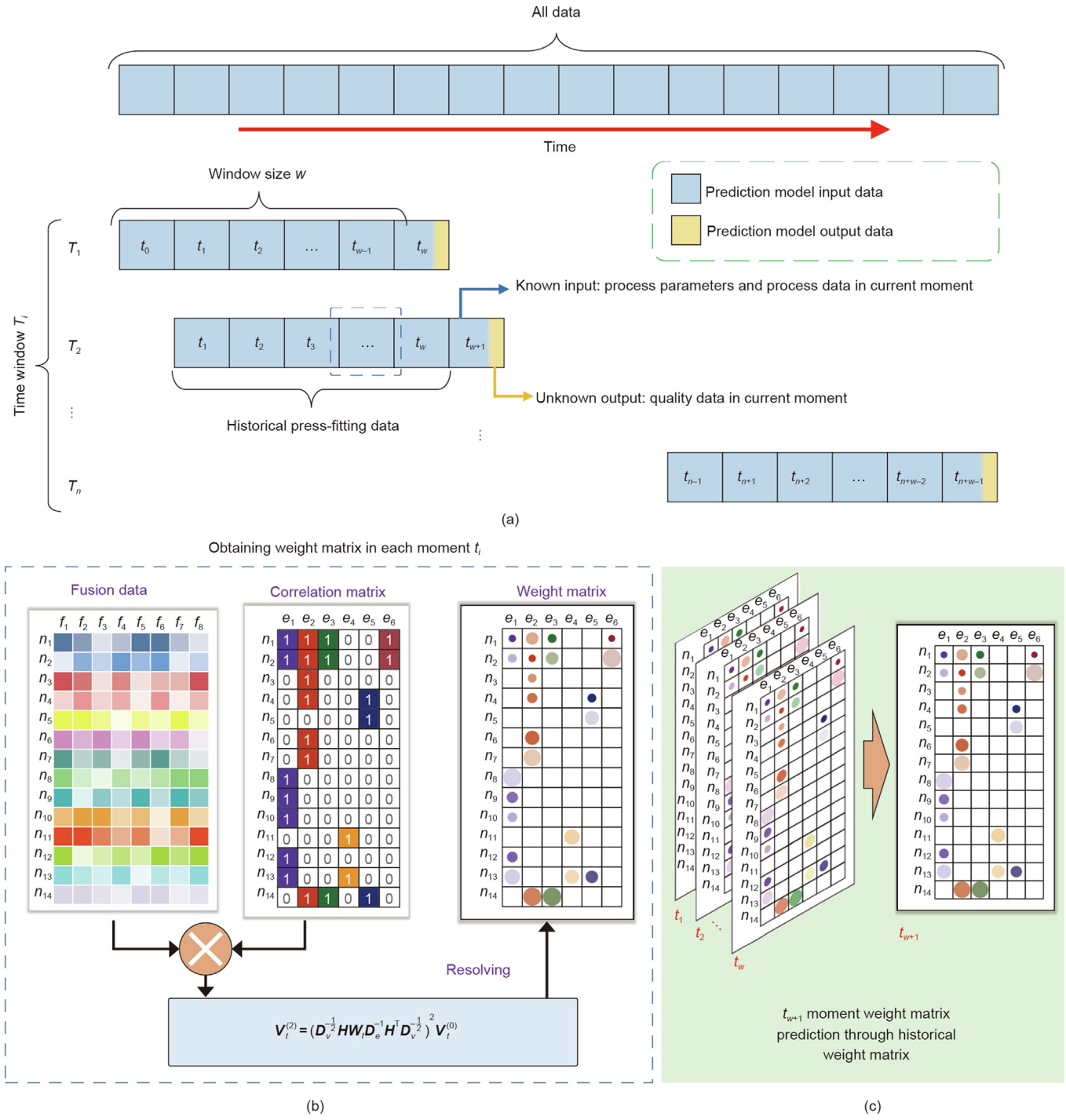

Fig. 6. Time series dataset of the QS-HGNN: (a) method of dataset construction; and (b, c) application of the dataset in QS-HGNN. f_i denotes the ith feature dimension of each node.

redundant hyperedge e_5, and removing multimodal nodes—demonstrated that the expert knowledge-based sparse topology outperforms indiscriminate full connection, with each hyperedge design making an irreplaceable contribution to model performance.

6. Digital twin deployment and online performance evaluation

6.1. Digital twin system

The QS-HGNN-based press-fitting process model is deployed into the twin intelligent press-fitting system to verify its effectiveness (Fig. 9). The system consists of a physical part on the right—the "twin intelligent press-fitting system"—and a digital part on the left—the "process system twin model." The physical part employs multi-source sensors to monitor key parameters of the press-fitting process in real time, including force, displacement, temperature, and visual information; the press-fitting results are evaluated through image analysis, providing feedback for the system. In the digital part, the global perception module receives and preprocesses multimodal data from the physical system, while the incremental decision-making framework, based on a recurrent structure, achieves dynamic decision optimization. The operation

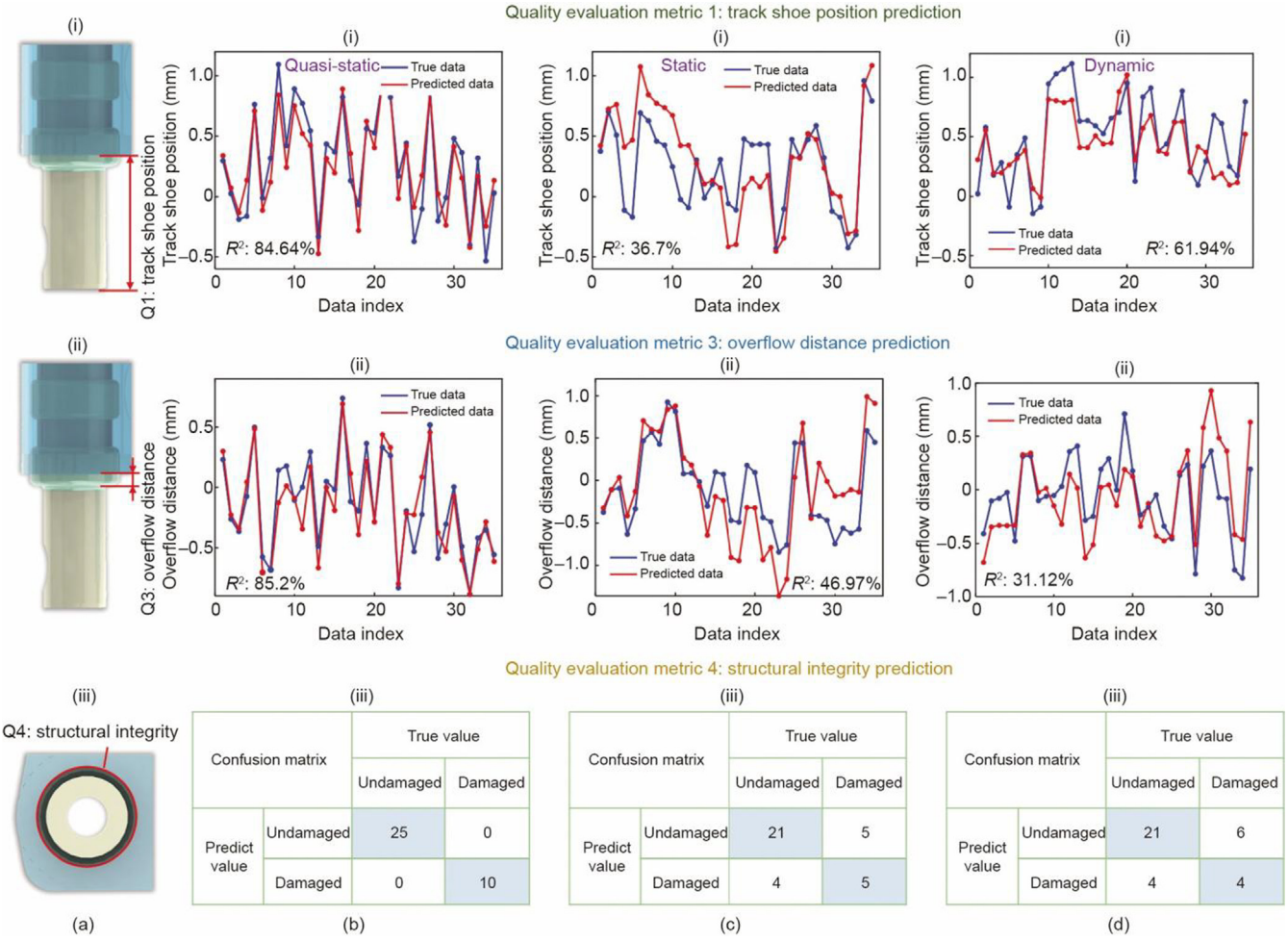

Fig. 7. Assembly quality prediction results of different hypergraph modeling strategies: (a-i)–(a-iii) quality indicator illustration; (b-i)–(b-iii) QS-HGNN; (c-i)–(c-iii) static HGNN; and (d-i)–(d-iii) dynamic HGNN. Rows correspond to track shoe position, overflow distance, and rubber bushing integrity, respectively.

of the twin intelligent press-fitting system follows a complete closed-loop mechanism comprising five key stages:

(1) Parameter acquisition stage: After loading the track pin, the industrial camera captures images to calculate the shaft diameter and pinhole diameter, while the temperature sensor collects environmental temperature, providing input conditions for subsequent process parameter optimization.

(2) Initial parameter optimization stage: The assembly quality optimization model generates preliminary press-fitting process parameters based on the input conditions and determines the optimal press-fitting velocity.

(3) Press-fitting execution stage: The main piezoelectric cylinder executes the press-fitting at the determined velocity; force and displacement sensors collect force–displacement data in real time, and the industrial camera captures key-frame images of the process.

(4) Dynamic parameter optimization stage: The system inputs the force–displacement curves and process images from the first six bushings into the optimization model for multimodal fusion analysis, outputting the over-press distance and back-press distance parameters for the final bushing. Due to a 5 s operation gap between completing the sixth bushing and starting the eighth, this time window suffices for data collection and processing without significant delay.

(5) Quality assessment and model update stage: After press-fitting is completed, quality assessment is performed, and the complete data are recorded into an incremental learning database. The model is periodically updated to enable continuous evolution, forming a complete closed-loop control system.

Digital twin systems in manufacturing are applied at various lifecycle stages. During system design and commissioning, digital twins are used for system validation and to identify inefficiencies before deployment [30]. In the system operation stage, they support performance monitoring and adaptive decision-making under long-term production conditions. The twin intelligent press-fitting system in this study targets the operation stage, modeling performance evolution due to accumulated process-related factors and enabling adaptive process parameter optimization during ongoing production.

6.2. Decision model and model update mechanism

In this study, the optimization stage is formulated as a model-based reverse decision process that utilizes the learned dynamic evolution model and also validates its effectiveness under evolving process conditions. Based on the aforementioned prediction model, the final assembly quality is influenced not only by static parameters (such as workpiece geometric parameters X_{geo} and environmental parameters X_{env}), but also by process variables. Therefore, the assembly quality q can be expressed as a multivariate function:

$$q = f_{\text{QS-HGNN}}\left(X_{\text{geo}}, X_{\text{env}}, v, p_g, p_f, d_o, d_b\right)_t \tag{24}$$

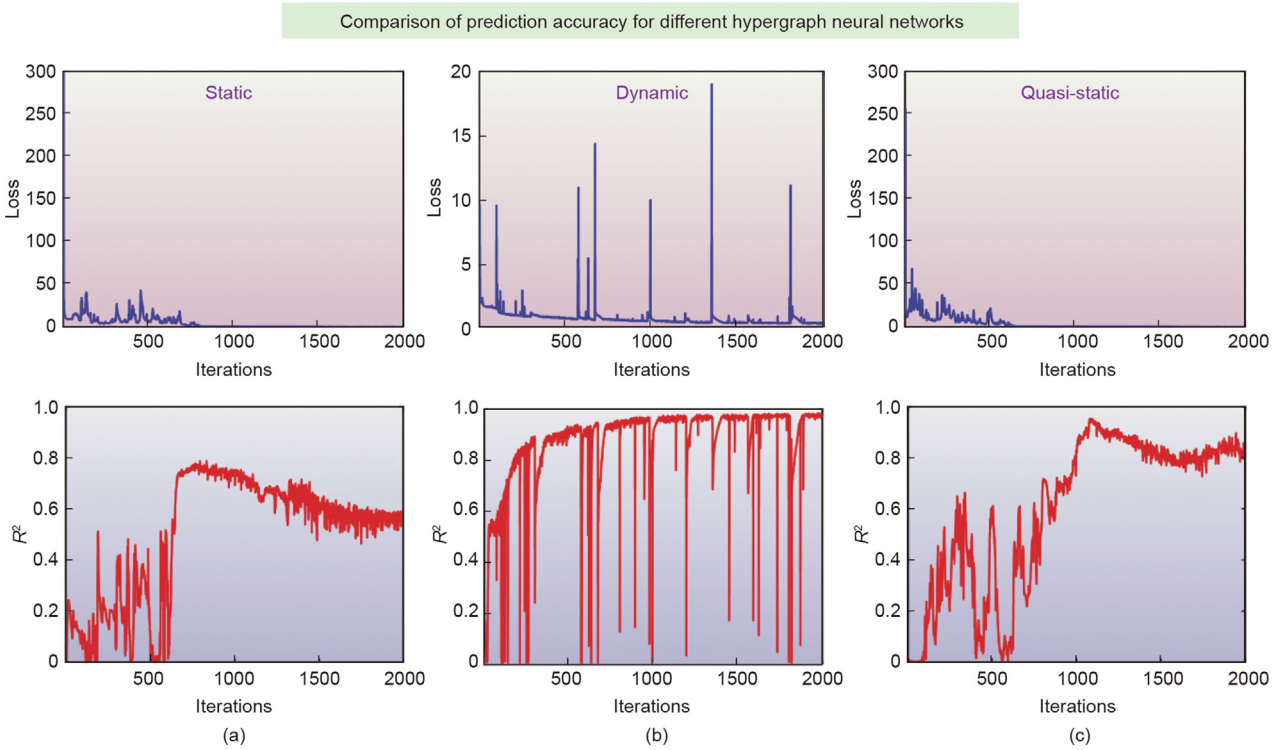

Fig. 8. Comparison of loss function and R^2 during training of three hypergraph networks: (a) static hypergraph; (b) dynamic hypergraph; and (c) quasi-static hypergraph.

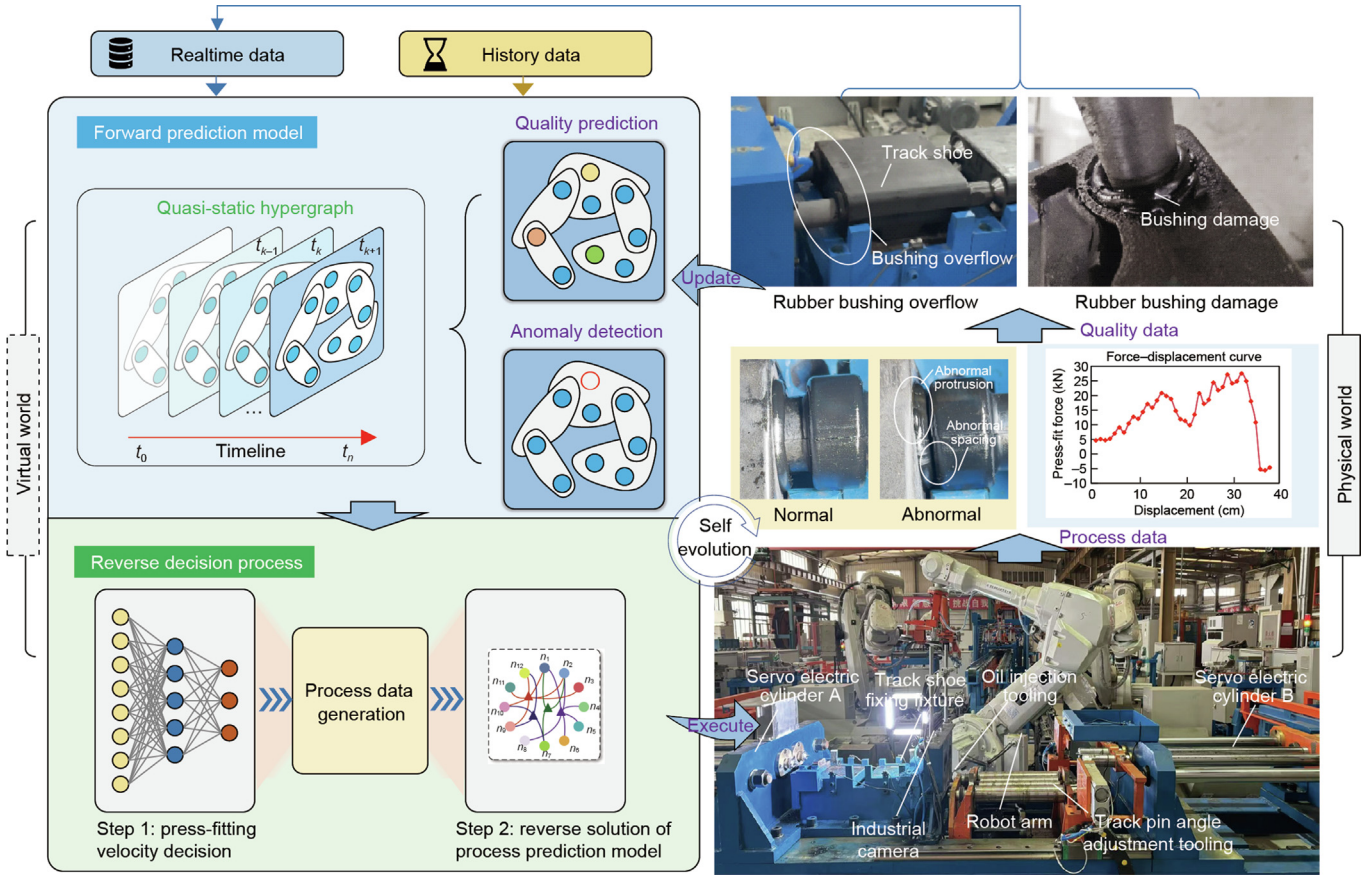

Fig. 9. Twin intelligent press-fitting system centered on quality prediction model. t_k denotes the kth time point.

where X_{geo} denotes the geometric parameters of the assembly, including the bushing diameter and the inner diameter of the track shoes, X_{env} represents the environmental parameter, including the environment temperature and press-fitting date, v represents the press-fitting velocity, $p = \{p_g, p_f\}$ collectively represents the process variables, including image information p_g and force–displacement curves p_f , and $d = \{d_o, d_b\}$ denotes the press-fitting displacement parameters, including the over-press distance d_o and back-press distance d_b.

To fully utilize the process variables gradually generated during the press-fitting process, this study proposes a stepwise decision strategy that divides the overall decision-making into two optimization stages (Fig. 10). Specifically, there are a total of 8 rubber bushings fixed on the track pin that need to be pressed sequentially. Before press-fitting begins, the model first makes an initial decision on the press-fitting velocity V_{ini} based on static parameters:

$$v_{ini} = f_{ini}(X_{geo}, X_{env})_t \tag{25}$$

where $f_{ini}(\cdot)$ is a lightweight multilayer perceptron (MLP) used to generate the initial press-fitting velocity from these static parameters.

Then, during the press-fitting execution, the system continuously collects press-fitting force–displacement curves and key-frame press-fitting images in real time. After completing the press-fitting of six bushings (used to accumulate sufficient process information), data collection is paused, and these observed intermediate process variables p are fed into the trained forward prediction model $f_{QS\text{-}HGNN}$. The final-stage process parameters, denoted by d, are determined by solving the following optimization problem:

$$d^* = \arg\min_d \| f_{QS\text{-}HGNN}(X_{geo}, X_{env}, v_{ini}, p, d)_t - y^* \|^2 \tag{26}$$

where y^* denotes the target assembly quality.

Based on these characteristics, this study adopts a combined reinforcement and incremental learning approach (Fig. S3 in Appendix A). The forward prediction layer models the mapping between process parameters and assembly quality, while the decision-making layer optimizes process parameters. A closed-loop optimization mechanism forms between the two layers through feedback from actual assembly quality: the improved accuracy of the prediction layer provides reliable decision support for the decision-making layer, and the optimization by the decision-making layer generates new data to enhance the prediction layer's performance. These components depend on each other and jointly influence the final optimization results.

The system adopts a "simulation-first, real-deployment-later" scheme: the decision model is first pre-trained in a virtual environment constructed by the QS-HGNN to generate simulated experiences $E_{sim}(s_t, a_t, r_t, s_t')$, where s_t denotes the assembly state at time t, a_t denotes the process parameters (action) selected by the policy function $\pi(a|s)$, r_t denotes the reward calculated by the value learning module, and s_t' denotes the resulting assembly state after executing a_t. Then deployed to the real system for fine-tuning using actual experiences $E_{real}(s_t, a_t, r_t, s_t')$. This approach significantly reduces raw material consumption while enabling efficient policy optimization.

As assembly equipment operates, the relationship between process parameters and quality dynamically evolves. An incremental learning mechanism iteratively updates the model by integrating new assembly data with historical data (indicated by the red solid arrow in Fig. S3 in Appendix A). A parameter-selective training strategy updates only selected key parameters in the base model while keeping the majority frozen to prevent catastrophic forgetting.

An experience replay buffer with FIFO updating and stratified sampling (30% recent, 70% historical) manages training data, combined with time-decay weighting and a performance monitoring mechanism that triggers early stopping and model rollback if validation performance degrades.

6.3. Model performance after deployment

A total of 63 press-fitting operations were conducted, and four key press-fitting quality indicators were recorded and analyzed: track shoe position, bushing position, presence of overflow, and presence of damage. The experiments were divided into two groups: ① baseline group: 27 press-fitting tests without optimization, serving as a reference for evaluating optimization effects; ② incremental optimization group: 36 press-fitting tests applying the incremental optimization model based on the QS-HGNN. To assess the effectiveness of the model update method for the digital twin system, incremental optimization experiments were completed over 6 working days, with 6 complete press-fitting tests conducted daily to evaluate the model's performance trend as data accumulated.

Based on the assembly quality indicators defined in Fig. 11(a), a comparative analysis using box plots evaluated the performance of the non-optimized and incremental optimization schemes on key assembly quality indicators (Fig. 11(b)). The results show that the incremental optimization scheme significantly improved assembly accuracy: the deviation of the track shoe position converged from a dispersed state under the non-optimized scheme to a concentrated distribution, the median deviation of the rubber bushing position approached –0.2 mm with reduced spread, and the amount of overflow was significantly controlled.

From the qualification rate statistics (Fig. 11(c)), the qualification rate for track shoe position increased from 70.3% to 100%; overflow status rose from 81.48% to 100%; and damage status improved from 88.89% to 100%. The qualification rate for rubber bushing position remained stable at 100% across all schemes, attributed to the elastic rebound deformation of the bushing that consistently returns it to a qualified position, indicating this parameter is insensitive to the optimization strategy. These results confirm the significant effect of the proposed method in enhancing overall system performance.

After deploying the model into the digital twin environment and updating it with new data, continuous performance improvement is achievable. As shown in Fig. 11(d), before applying the proposed method, the accuracy of track shoe position and overflow indicators fluctuated greatly with a probability of failure; after model deployment and continuous updating, all quality indicators stabilized, and overall assembly quality significantly improved. This confirms the model's effectiveness in adapting to changes in the production environment and achieving continuous improvement in assembly quality.

These experimental results demonstrate that deploying the proposed process quality prediction model in the twin intelligent press-fit system yields clear superiority across multiple key indicators, proving the model's adaptability and sustained optimization performance in dynamic production environments.

6.4. Discussion on the generalizability of the modeling method

The proposed QS-HGNN is applicable not only to the rubber bushing press-fitting system but also exhibits broad generalizability, extending to various manufacturing process systems and industrial scenarios. Progressive performance evolution phenomena, such as equipment wear, material aging, and environmental fluctuations, are common in manufacturing systems. The QS-HGNN's quasi-static assumption (microscopically static, macro-

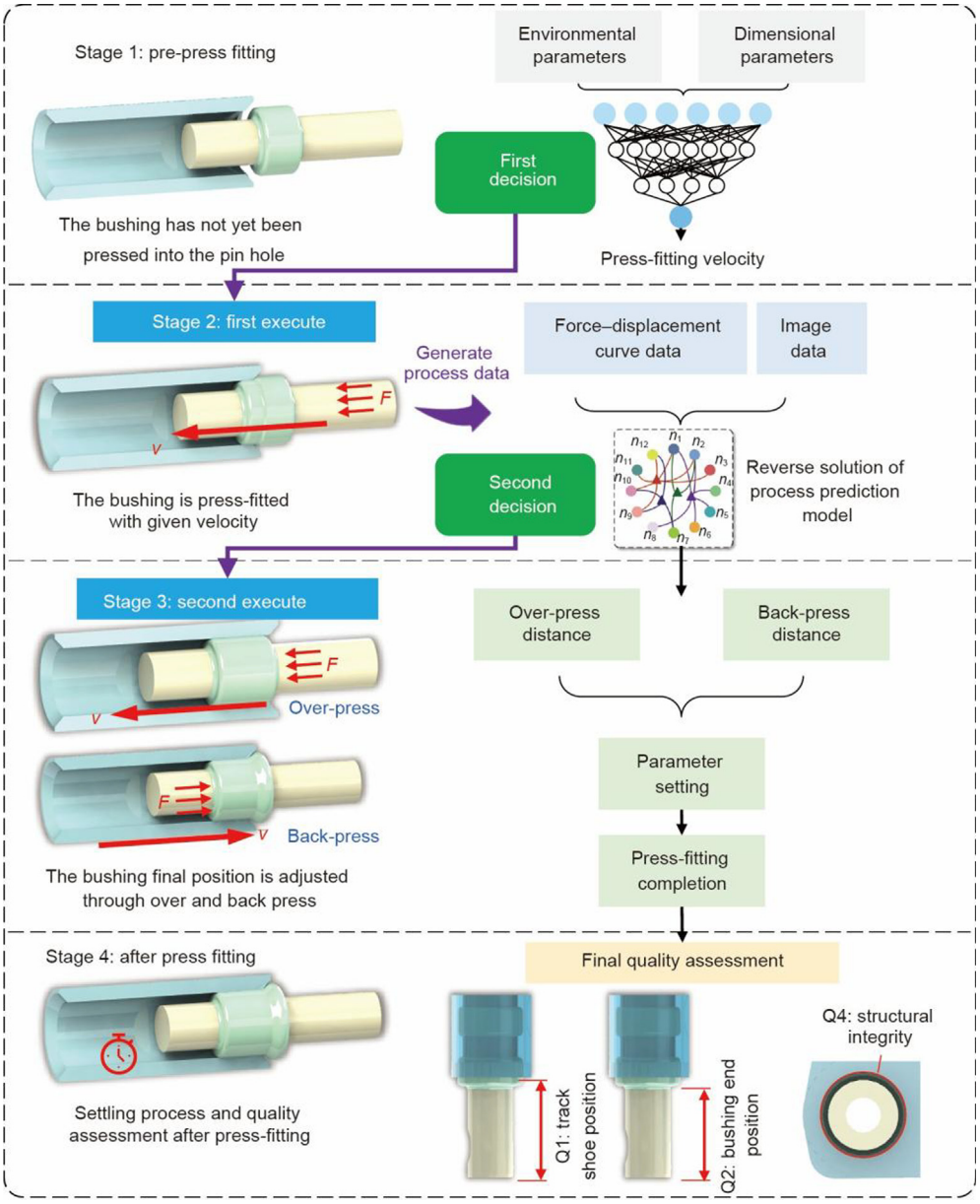

Fig. 10. Press-fitting process parameter decision based on quality prediction model.

scopically dynamic) aligns well with these time-varying characteristics. In scenarios such as metal cutting, injection molding, and welding processes, the correlation strength between process parameters and quality indicators typically changes gradually. QS-HGNN effectively captures these evolving patterns through discretized weight matrix solving and LSTM-based temporal modeling. Additionally, the hypergraph structure of QS-HGNN can flexibly incorporate domain knowledge, explicitly representing multi-factor coupling relationships. This makes it suitable for complex process systems, such as multi-step collaborative assembly and composite material forming, thereby preventing information loss associated with traditional flat neural networks that overlook higher-order interactions. Its superior performance under small-sample conditions makes it particularly advantageous for high-cost industrial applications with limited data volumes, such as aerospace-critical component manufacturing. In the future, QS-HGNN can be extended to scenarios such as equipment health management, where its "structurally stable + dynamically weighted" modeling framework provides a universal paradigm for intelligent modeling of dynamic systems.

7. Conclusions

This study addresses challenges in dynamic performance evolution and small-sample data modeling in manufacturing process systems by proposing a QS-HGNN modeling approach, validated through its application to the rubber bushing press-fitting system. The main conclusions are as follows:

(1) This study proposes a quasi-static assumption of "microscopic static–macroscopic evolution" for manufacturing process system performance. Based on this assumption, a QS-HGNN modeling method is developed. This method explicitly represents multivariate correlations among process parameters through a hypergraph structure, achieves spatial correlation modeling via discretized weight matrix solving, and captures temporal evolution with an LSTM temporal mechanism. It effectively balances model

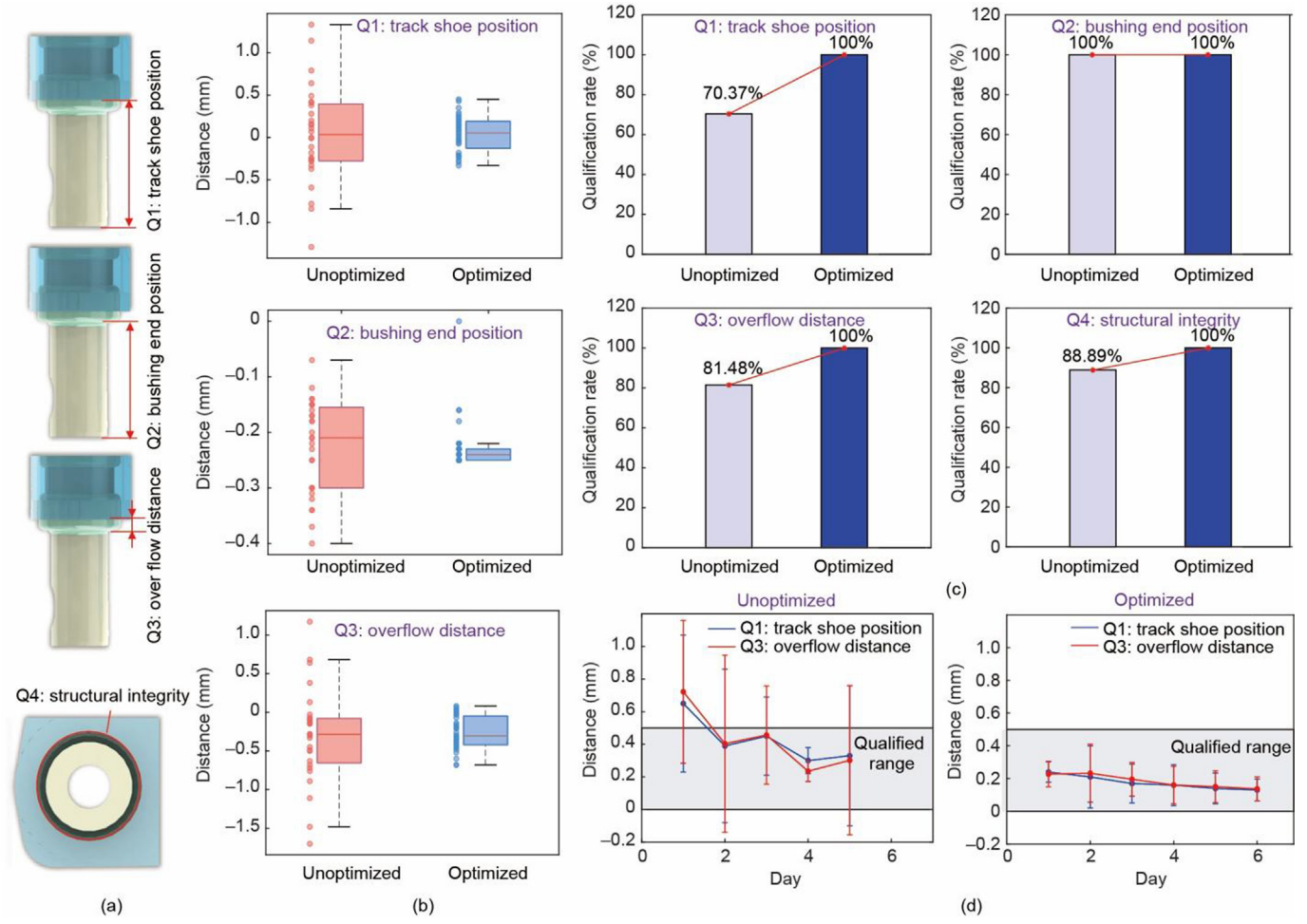

Fig. 11. Comparison of process quality before and after deploying the quality prediction model into the digital twin intelligent press-fitting system: (a) quality indicator illustration; (b) comparison of three quality indicators; (c) comparison of pass rates; (d) variation of process quality over the days of operation.

complexity and accuracy, overcoming traditional dynamic models' dependence on large datasets.

(2) The modeling approach is validated on the rubber bushing press-fitting process of tracked vehicles. A multimodal data processing method integrates force–displacement curves, image data, and process parameters. By introducing PINN constraints, the model's generalization ability under small-sample conditions is enhanced. Training with process parameters, variables, and quality data from the rubber bushing press-fitting process, comparative studies demonstrate that QS-HGNN achieves higher modeling accuracy than traditional static and dynamic hypergraph networks. The loss curve shows that QS-HGNN maintains a stable training process while achieving a lower final loss value, exhibiting excellent convergence performance.

(3) The QS-HGNN model is deployed in an intelligent digital twin system for rubber bushing press-fitting. Centered on the quality prediction model proposed here, the system enables dynamic optimization of process parameters based on QS-HGNN through incremental learning, forming a complete closed loop from prediction modeling to process optimization and model updating. Experimental results show that after process optimization using this method, the dispersion of key product quality indicators decreases by 40%, and the quality pass rate improves from 70.3% to 100%, verifying the effectiveness and practicality of the QS-HGNN method in manufacturing process system modeling and optimization.

In summary, the QS-HGNN modeling method proposed in this study provides a novel theoretical approach for digital twin modeling of manufacturing process systems with dynamic performance evolution and offers a feasible technical solution to the challenge of small-sample dynamic modeling in industrial scenarios. This work holds significant theoretical and practical value for advancing the field of intelligent manufacturing.

CRediT authorship contribution statement

Yiru Chen: Writing – original draft, Data curation. **Peiyuan Ding:** Writing – original draft, Validation. **Jianfu Zhang:** Resources. **Pingfa Feng:** Formal analysis. **Xiangyu Zhang:** Project administration. **Jianjian Wang:** Writing – review & editing, Conceptualization.

Declaration of competing interest

The authors declare that they have no known competing financial interests or personal relationships that could have appeared to influence the work reported in this paper.

Acknowledgments

We gratefully acknowledge the financial support from the National Natural Science Foundation of China (52475470).

Appendix A. Supplementary material

Supplementary data to this article can be found online at https://doi.org/10.1016/j.eng.2026.03.012.

References

[1] Qi Q, Tao F. Digital twin and big data towards smart manufacturing and industry 4.0: 360 degree comparison. IEEE Access 2018;6:3585–93.
[2] Tao F, Zhang H, Liu A, Nee AY. Digital twin in industry: state-of-the-art. IEEE Trans Industr Inform 2019;15(4):2405–15.
[3] Kang HS, Lee JY, Choi S, Kim H, Park JH, Son JY, et al. Smart manufacturing: past research, present findings, and future directions. Int J Precis Eng Manuf-Green Technol 2016;3(1):111–28.
[4] Montgomery DC. Design and analysis of experiments. 10th ed. Hoboken: John wiley & sons; 2017.
[5] Psarommatis F, May G, Dreyfus PA, Kiritsis D. Zero defect manufacturing: state-of-the-art review, shortcomings and future directions in research. Int J Prod Res 2020;58(1):1–17.
[6] Wang Q, Ma Y, Zhao K, Tian Y. A comprehensive survey of loss functions in machine learning. Ann Data Sci 2022;9(2):187–212.
[7] Lu Y. Industry 4.0: a survey on technologies, applications and open research issues. J Ind Inf Integr 2017;6:1–10.
[8] Zhong RY, Xu X, Klotz E, Newman ST. Intelligent manufacturing in the context of industry 4.0: a review. Engineering 2017;3(5):616–30.
[9] Uhlemann THJ, Lehmann C, Steinhilper R. The digital twin: realizing the cyber-physical production system for industry 4.0. Procedia CIRP 2017;61:335–40.
[10] Sick B. On-line and indirect tool wear monitoring in turning with artificial neural networks: a review of more than a decade of research. Mech Syst Signal Process 2002;16(4):487–546.
[11] Teti R, Jemielniak K, O'Donnell G, Dornfeld D. Advanced monitoring of machining operations. CIRP Ann 2010;59(2):717–39.
[12] Zhou Y, Xue W. Review of tool condition monitoring methods in milling processes. Int J Adv Manuf Technol 2018;96(5–8):2509–23.
[13] Lei Y, Li N, Guo L, Li N, Yan T, Lin J. Machinery health prognostics: a systematic review from data acquisition to RUL prediction. Mech Syst Signal Process 2018;104:799–834.
[14] Si XS, Wang W, Hu CH, Zhou DH. Remaining useful life estimation–a review on the statistical data driven approaches. Eur J Oper Res 2011;213(1):1–14.
[15] Dimla DE. Sensor signals for tool-wear monitoring in metal cutting operations—a review of methods. Int J Mach Tools Manuf 2000;40(8):1073–98.
[16] Hornik K, Stinchcombe M, White H. Multilayer feedforward networks are universal approximators. Neural Netw 1989;2(5):359–66.
[17] LeCun Y, Bengio Y, Hinton G. Deep learning. Nature 2015;521(7553):436–44.
[18] Tercan H, Meisen T. Machine learning and deep learning based predictive quality in manufacturing: a systematic review. J Intell Manuf 2022;33(7):1879–905.
[19] Feng Y, You H, Zhang Z, Ji R, Gao Y. Hypergraph neural networks. Proc AAAI Conf Artif Intell 2019;33(1):3558–65.
[20] Gao Y, Zhang Z, Lin H, Zhao X, Du S, Zou C. Hypergraph learning: methods and practices. IEEE Trans Pattern Anal Mach Intell 2022;44(5):2548–66.
[21] Raissi M, Perdikaris P, Karniadakis GE. Physics-informed neural networks: a deep learning framework for solving forward and inverse problems involving nonlinear partial differential equations. J Comput Phys 2019;378:686–707.
[22] Jiang J, Wei Y, Feng Y, Cao J, Gao Y. Dynamic hypergraph neural networks. In: Proceedings of the 28th International Joint Conference on Artificial Intelligence; 2019 Aug 10–16; Macao, China. Palo Alto: AAAI Press; 2019. p. 2635–41.
[23] Pareja A, Domeniconi G, Chen J, Ma T, Suzumura T, Kanezashi H, et al. EvolveGCN: evolving graph convolutional networks for dynamic graphs. Proc AAAI Conf Artif Intell 2020;34(4):5363–70.
[24] Hamilton WL, Ying R, Leskovec J. Inductive representation learning on large graphs. In: Proceedings of the 31st International Conference on Neural Information Processing Systems; 2017 Dec 4–9; Long Beach, CA, USA. New York City: Curran Associates Inc.; 2017. p. 1025–35.
[25] Zeng H, Zhou H, Srivastava A, Kannan R, Prasanna V. GraphSAINT: graph sampling based inductive learning method. 2020. arXiv:1907.04931.
[26] Chen Y, Zhang J, Feng P, Zheng Z, Zhang X, Wang J. A novel constitutive model of carbon black rubber for the numerical analysis of press-fitting of rubber bushing. J Rubber Res 2025;28:105–17.
[27] Chen Y, Zhang J, Feng P, Zheng Z, Zhang X, Wang J. Development of a cascaded multitask physics-informed neural network (CM-PINN) to construct the muti-physical field model of rubber bushing press fitting. J Intell Manuf 2025;36:3607–24.
[28] Leng J, Su X, Liu Z, Zhou L, Chen C, Guo X, et al. Diffusion model-driven smart design and manufacturing: prospects and challenges. J Manuf Syst 2025;82:561–77.
[29] Leng J, Zuo K, Xu C, Zhou X, Zheng S, Kang J, et al. Physics-informed machine learning in intelligent manufacturing: a review. J Intell Manuf 2025. in press.
[30] Leng J, Zhou M, Xiao Y, Zhang H, Liu Q, Shen W, et al. Digital twins-based remote semi-physical commissioning of flow-type smart manufacturing systems. J Clean Prod 2021;306:127278.